Structure of Triazadienyl Fluoride, FN_3, by Microwave, Infrared, and ab Initio Methods

D. Christen,*† H. G. Mack,† G. Schatte,‡ and H. Willner‡

Contribution from the Institut für Physikalische und Theoretische Chemie, Universität Tübingen, D-7400 Tübingen, and Institut für Anorganische Chemie, Universität Hannover, D-3000 Hanover, Federal Republic of Germany. *Received June 1, 1987*

Abstract: Microwave and infrared spectra of the unstable species FN_3 as well as its various ^{15}N-enriched isotopomers have been recorded and analyzed, yielding data on molecular structure, dipole moment, and harmonic force constants. The rotational constants for the parent isotopic species are (in MHz) $A = 48\,131.448$, $B = 5713.288$, $C = 5095.276$. The dipole moments (D) are $\mu_a = 1.1$, $\mu_b = 0.7$, $\mu_{total} = 1.3$. The fundamental frequencies (cm^{-1}) are 2037, 1090, 873.5, 658, 241, 504. The diagonal force constants (100 N/m) are $f_{N_\beta N_\omega} = 17.414$, $f_{N_\alpha N_\beta} = 6.686$, $f_{N_\alpha F} = 3.753$, $f_{FN_\alpha N_\beta} = 1.245$, $f_{N_\beta N_\beta N_\omega} = 0.477$, $f_{oop} = 0.014$. The structural parameters are $r_{NF} = 144.4$, $r_{N_\alpha N_\beta} = 125.3$, $r_{N_\beta N_\omega} = 113.2$ pm; $\angle FN_\alpha N_\beta = 103.8°$, $\angle N_\alpha N_\beta N_\omega = 170.9°$. Ab initio calculations using 6-31G* and MP2/6-31G* basis sets have been carried out to calculate structure, force field, dipole moment, and electric field gradients at the ^{14}N quadrupole nuclei.

Triazadienyl fluoride is one of the most explosive and thermally unstable covalent azides known, and consequently no complete structural or spectroscopic investigations of this molecule have been published until now. All that was known were some theoretical calculations of structural parameters[1,2] and argon-matrix IR frequencies of a few of the fundamental vibrations.[3] The recent discovery of a relatively safe synthetic route to the pure substance[4] has opened the way for microwave and IR spectroscopic investigations of the substance in the gas phase and also made the synthesis of the ^{15}N-substituted triazadienyl fluorides feasable, which in turn allowed for a complete determination of the structure and harmonic force field. The results are compared with MP2/6-31G* ab initio calculations that also guided the search for the harmonic force field.

Experimental Section

Warning! Triazadienyl fluoride is extremely explosive in the liquid and solid states. We recommend 20 mg as the absolute maximum amount of sample to be handled in one batch.

The synthetic route to pure FN_3 is described in ref 4. The main step is the reaction of HN_3 with F_2; thus for the synthesis of ^{15}N-enriched species (N_α, N_β, N_ω) one needs correspondingly enriched NaN_3, which was obtained in the following way. In a 100-mL glass vessel with a Teflon stopcock, 40 mg (1.8 mmol) of Na and 3.5 mmol of $^{15}NH_3$ (95%, A. Hempel GmbH, Düsseldorf) were reacted for 2 h at 350 °C to yield $Na^{15}NH_2$. The evolving hydrogen was pumped through a cold trap kept at −196 °C to recover excess $^{15}NH_3$. Thereafter, 2 mmol of N_2O was condensed into the vessel, and the mixture was heated to 150 °C for 12 h. The $Na^{15}NNN$ that was formed was dissolved in water, filtered, and neutralized (pH 9) with dilute H_2SO_4 before it was dried at 90 °C. The terminal nitrogens are equivalent in ionic azides; thus $Na^{15}NNN$ is the precursor of both $F^{15}NNN$ and $FNN^{15}N$. In order to substitute the central nitrogen in NaNNN with ^{15}N, 1.2 mmol of $NaNH_2$ was reacted with 1 mmol of ^{15}NNO (98%, A. Hempel GmbH, Düsseldorf) as described above. The microwave and IR matrix investigation showed that small amounts (<10%) of $Na^{15}NNN$ must also be formed by this reaction.

Microwave Spectroscopy. Three batches of gaseous sample, kept at dry ice temperatures, were at various times transported from Hannover to Tübingen in order to record the microwave spectra, using a conventional 100-kHz Stark modulated spectrometer in X, K, and Q band, flowing the sample (-80 °C) through the aluminum cell, cooled to -60 °C, while maintaining a pressure of 0.1–2 Pa.

Vibrational Spectroscopy. The IR spectra of FN_3 in the gas phase (glass cuvette, 20 cm optical path length, KBr and TPX windows) were recorded at ambient temperatures, using two FTIR spectrometers: MXS (Nicolet; resolution, 4 cm^{-1}) and IFS 113 (Bruker, resolution, 0.05 cm^{-1}). IR spectra of FN_3 trapped in an Ar matrix were recorded, using the set-up described in ref 5.

Results

Microwave Spectroscopy. FN_3 is a near-prolate rotor, expected to possess its major dipole moment component along the A axis. Therefore, a broad-band spectrum in K band, sweeping the Marconi Sweeper 6600A from 18 to 26.5 GHz in steps of 3 MHz in half an hour by applying a 0–20-V ramp voltage to the external sweep input connector, was recorded at the very beginning, immediately revealing three groups of lines centered around 21.6 GHz, which model calculations showed must be the (ground and vibrationally excited states) μ_a-type $K = 0$ and 1, $J = 1$–2 transitions of FN_3. Consequently, the microwave spectroscopic investigation was concentrated on these lines as well as a few others that could be safely predicted, using the preliminary rotational constants, derived from the analysis of these three lines. (With such an unstable molecule, one wants to know what one is looking at.)

The assignment of the 1–2 μ_a transitions was straightforward, the only complication arising from the many vibrationally excited-state lines, first and foremost the FNN-bending vibration, ν_5. The situation only became really difficult in the higher J, higher K regions, where almost all lines are overlapped. An impression of the multitude of excited states is given by Figure 1, which shows the well-isolated 3_{12}–4_{13} transition, where at least 12 different vibrational states of the normal species can be identified together with the ground-state lines of some ^{15}N-substituted species (natural abundance, 0.34%). All these lines have their Stark shift toward lower frequency ($3_{12}4_{13}$ being the upper part of the $K = 1$ doublet), but intermingled with the many $3_{12}4_{13}$ are a few lines with a different Stark effect. These very weak lines are μ_b transitions of the ground state of the normal species, but these lines are so weak that they could only be unambigously identified for the ground state of the main species.

The recording of the spectra of the ^{15}N-enriched species proceeded parallel to the investigation of the normal species, except that because of a shortage of substance, less lines were measured (and except for one μ_b line in ^{15}N-triazadienyl fluoride, they were all of μ_a type). So for the analysis of these spectra, assumptions of inertial defects and centrifugal distortion had to be made.

Centrifugal Distortion Analysis. The measured transitions were used to derive rotational and centrifugal distortion constants, using the first-order Watson Hamiltonian in the A reduction.[6] FN_3 is a planar, near-prolate rotor, and it was necessary to fix δ_K to

† University of Tübingen.
‡ University of Hannover.

(1) Clidewell, Ch.; Holden, H. D. *J. Mol. Struct.* **1982**, *90*, 131.
(2) Peters, N. J. S. Dissertation, Princeton University, 1982.
(3) Milligan, D. E.; Jacox, M. E. *J. Chem. Phys.* **1964**, *40*, 2461.
(4) Gholivand, K.; Schatte, G.; Willner, H. *Inorg. Chem.* **1987**, *26*, 2137.
(5) Willner, H. *Z. Anorg. Allg. Chem.* **1981**, *481*, 117.
(6) Watson, J. K. G. In *Vibrational Spectra and Structure*; Durig, J. R., Ed.; Elsevier: Amsterdam, 1977; pp 1–89.

0002-7863/88/1510-0707$01.50/0

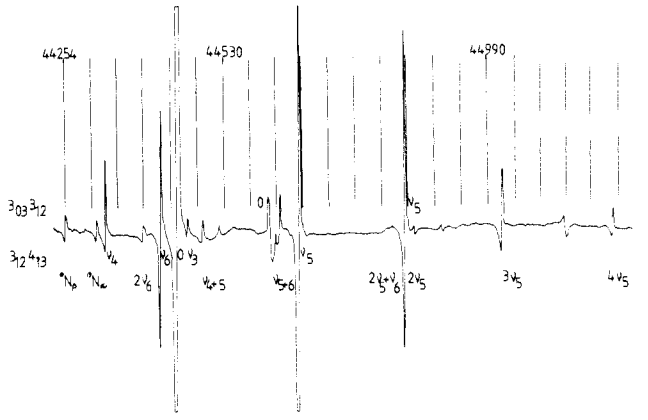

Figure 1. The rotational transition 3_{12}–4_{13} in FN_3 around 44 GHz, showing the population of the vibrational ground state as well as 11 vibrationally excited states and two ^{15}N species (in natural abundance). A few lines with stark shift to higher frequency have also been identified; they are the 3_{03}–3_{12} μ_b transitions in the ground and $v_5 = 1$ states. (Pressure, 3 Pa, flowing; temp., −60 °C; time constant, 300 ms; Stark field, 1000 V/cm).

the value calculated from the harmonic force field for the ground state of the normal species. Because of the lack of μ_b lines for most vibrationally excited states as well as ^{15}N-substituted species (except for $^{15}N_\beta$), a number of parameters had to be fixed in these calculations. These parameters are indicated in Table I. The A rotational constant was always fixed to a value reproducing the inertial defect as calculated from the harmonic force field for the species where no μ_b lines were measured. All measured transitions are collected in Table II.

Nuclear Quadrupole Interaction. Triazadienyl fluoride contains three nonequivalent nitrogen nuclei and, therefore, the microwave lines show complicated hyperfine structures which were rarely fully resolved. From the measurements on ^{15}N-substituted species, it is obvious that the quadrupole coupling constants for the nitrogen at the α position are much bigger than those at the other two positions, but further analysis must await a high-resolution study of the 0–1 transitions of the different isotopomers, which we are planning to do in the near future (see also the section on ab initio calculations).

Molecular Structure. The first structural information on FN_3 is found from the inertial defect (see Table I), which (small and positive) proves the molecule to be planar. Only the normal coordinate analysis yields an unequivocal proof of the planarity of FN_3, for example, by reproducing the changes in the inertial defect upon excitation of different vibrational modes, but since ν_5, the FNN bending vibration, is the only one below 500 cm^{-1}, it is going to have a major influence on the size of the inertial defect (id). An extrapolation of the inertial defects from $v_5 = 1$ (id = 0.545) over v_0 (id = 0.229) to $v_5 = -1/2$ (the hypothetical "FNN frozen state") yields id($v_5 = -1/2$) = 0.071, very close to 0, the value expected for a perfectly rigid, planar molecule. Thus the molecular structure is described with six parameters, and it is necessary to know the rotational constants of at least three isotopomers. Because of the planarity, each isotopomer yields only two independent structural data.

In order to derive a trustworthy structure, at least one more isotopic species is needed, so the structure determined here is based on the rotational constants of the normal species and each of the ^{15}N-substituted isotopomers. The most reliable structure of a molecule with a long (NNN) chain fragment and considerable vibrational contributions to the rotational constants seems to be a substitution structure calculated via the Kraitchman coordinates.[7] Since fluorine possesses only one stable isotope, the fluorine coordinates must be determined from the center-of-mass conditions. The coordinates and structure are shown in Table III. The uncertainties on the structural parameters have been estimated and should include the effect of using the center-of-mass conditions as well as covering the uncertainty in the small b coordinate of the central nitrogen.

(7) Kraitchman, J *Am. J. Phys.* **1953**, *21*, 17.

Table I. Rotational and Centrifugal Distortion Constants (MHz) in FN_3, Inertial Defects (u Å^2), and Vibration/Rotation Parameters (MHz)

	normal species gr state	$F^{15}NNN$ gr state	$FN^{15}NN$ gr state	$FNN^{15}N$ gr state
A	48131.448 (171)	46102.300[a]	48082.445 (663)	47848.353[a]
B	5713.288 (84)	5699.980 (22)	5686.522 (71)	5530.821 (168)
C	5095.276 (58)	5061.161 (22)	5073.343 (58)	4946.517 (254)
Δ_J	0.0024 (8)	0.0025 (4)	0.0024 (17)	0.0024[a]
Δ_{JK}	−0.1465 (17)	−0.1272 (13)	−0.1287 (442)	−0.1465[a]
Δ_K	3.2881 (1553)	3.2881[a]	3.2881[a]	3.2881[a]
δ_J	0.0009 (12)	0.0011 (5)	0.0009[a]	0.0009[a]
δ_K	0.0348[a]	0.0348[a]	0.0348[a]	0.0348[a]
id	0.229	0.229[a]	0.231	0.229[a]
	$v_5 = 1$	$v_5 = 1$	$v_5 = 1$	$v_5 = 1$
A	48335.665 (365)	46309.759[a]	48319.969[a]	48008.638[a]
B	5743.118 (89)	5729.238	5715.430 (19)	5559.762
C	5104.959 (89)	5070.422	5082.698 (29)	4955.948
Δ_J	0.0029 (12)	0.0024[a]	0.0024[a]	0.0024[a]
Δ_{JK}	−0.1435 (33)	−0.1465[a]	−0.1465[a]	−0.1465[a]
Δ_K	3.2881[a]	3.2881[a]	3.2881[a]	3.2881[a]
δ_J	0.0027 (17)	0.0009[a]	0.0009[a]	0.0009[a]
δ_K	0.0348[a]	0.0348[a]	0.0348[a]	0.0348[a]
id	0.545	0.548[a]	0.548[a]	0.548[a]
α^A	204.217	207.459	237.524	160.285
α^B	29.830	29.258	28.908	28.941
α^C	9.683	9.261	9.355	9.413

	normal species $v_5 = 2$	$FN^{15}NN$ $v_5 = 2$
A	48689.193[a]	48727.043[a]
B	5771.542 (42)	5742.610
C	5114.496 (43)	5092.199
Δ_J	0.0039 (6)	0.0024[a]
Δ_{JK}	−0.1432 (16)	−0.1465[a]
Δ_K	3.2881[a]	3.2881[a]
δ_J	0.0014 (8)	0.0009[a]
δ_K	0.0348[a]	0.0348[a]
id	0.869[a]	0.869[a]

[a] Fixed in the least-squares fit.

Dipole Moment. Quantitative Stark effect studies were made on a selection of μ_a and one μ_b transitions of FN_3. The voltmeter of the square-wave generator was calibrated against the Stark shifts of the 1–2 transition of OCS (dipole moment: 0.71519 D[8]) with the absorption cell at −60 °C. The Stark effect is complicated because of the interaction of the quadrupole moments with the static electric field, but the transitions selected can (at the voltages applied) be described as high-field cases (see, e.g., ref 9). Observed Stark shifts are given in Table IV, as is the resulting dipole moment.

Vibrational Spectra and Normal Coordinate Analysis. The frequencies of all recorded vibrations of gaseous or matrix-isolated FN_3 as well as its ^{15}N-enriched isotopomers have been collected in Table V. The irreducible representations of the vibrations of the planar FN_3 molecule (C_s symmetry) are:

$$\Gamma_{vib} = 5a' \text{ (IR, Ra p)} + 1a'' \text{ (IR, Ra dp)}$$

The assignment according to representation and approximate mode description for the six fundamentals has already been published in ref 4 but is reproduced in Table V.

From Tables V and VI, it is obvious that the fundamentals ν_1 and ν_3 are perturbed through anharmonic resonance with combination and overtones of other fundamentals. ν_1 is perturbed by $2\nu_2$ and $(\nu_2 + \nu_3)$, respectively, and ν_3 is perturbed by $(\nu_4 + \nu_5)$. The greatest perturbations of ν_1 are experienced in the $F^{15}NNN$ species (through $2\nu_2$) and in the $FN^{15}NN$ species (through $\nu_2 + \nu_3$). ν_3 experiences its greatest perturbation from $(\nu_4 + \nu_5)$ in the $FN^{15}NN$ species.

Knowledge of the unperturbed frequencies, however, is a prerequisite for the normal coordinate analysis. Thus we have

(8) Muenter, J. S. *J. Chem. Phys.* **1968**, *48*, 4544–4547.
(9) Gordy, W.; Cook, R. L. *Microwave Molecular Spectra*; *Interscience*: New York, 1970; pp 316–319.

Table II. Measured Rotational Transitions in FN_3 (MHz)[a]

	normal species			$^{15}N_\alpha$		$^{15}N_\beta$			$^{15}N_\omega$	
	gr state	$v_5 = 1$	$v_5 = 2$	gr state	$v_5 = 1$	gr state	$v_5 = 1$	$v_5 = 2$	gr state	$v_5 = 1$
$0_{00} \rightarrow 1_{01}$	10808.50	10847.90		10761.19	10799.65	10759.72			10477.05	10515.70
$1_{11} \rightarrow 2_{11}$	20999.74	21058.70	21115.60	20884.06	20941.18	20907.13	20964.14			
$1_{01} \rightarrow 2_{02}$	21610.44	21689.03	21764.58	21514.67		21513.12	21589.26	21662.22	20948.73	
$1_{10} \rightarrow 2_{11}$		22334.59	22429.33	22161.35		22133.22			21539.35	21635.60
$3_{03} \rightarrow 4_{04}$	43166.67	43320.66	43468.42							
$3_{22} \rightarrow 4_{23}$	43233.04	43390.61	43541.90	43042.20						
$3_3 \rightarrow 4_3$	43257.44	43416.03	43568.26	43068.16						
$3_{21} \rightarrow 4_{22}$	43300.18	43461.40	43616.65	43117.17						
$3_{12} \rightarrow 4_{13}$	44456.85	44653.72	44842.65	44306.36		44252.59	44444.10	44625.53		
$2_{02} \rightarrow 2_{11}$	43658.30									
$3_{03} \rightarrow 3_{12}$	44608.36	44854.80				44568.72				
$4_{04} \rightarrow 4_{13}$	45898.50									
$6_{15} \rightarrow 7_{16}$	43987.20									

[a] In addition, the $3_{12} \rightarrow 4_{13}$ transition has been measured for the following vibrationally excited states: $v_5 = 3$, 45023.71; $v_5 = 4$, 45196.06; $v_6 = 1$, 44422.30; $v_4 = 1$, 44323.00; $v_5 = 1$, $v_6 = 1$, 44625.33; $v_5 = 1$, $v_4 = 1$, 44511.83; $v_5 = 2$, $v_6 = 1$, 44819.80; $v_3 = 1$, 44477.68.

Table III. Kraitchman Coordinates and Structures of FN_3[a]

	a	*b*		
F	−141.371	39.483	$N_\alpha F$	144.4 (1.0)
N_α	−45.747	−68.727	$N_\alpha N_\beta$	125.3 (1.0)
N_β	65.143	−10.472	$N_\beta N_\omega$	113.2 (1.0)
N_ω	172.406	25.631	$FN_\alpha N_\beta$	103.8 (0.5)
			$N_\alpha N_\beta N_\omega$	170.9 (1.0)

[a] Units in pm and deg.

Table IV. Stark Shifts and Derived Dipole Moment Components of FN_3[a]

		species	Stark field (V/cm)	Stark shift (MHz)
$0_{00} \rightarrow 1_{01}$	M = 0	$^{15}N_\beta$	1040	16.90
		$^{15}N_\alpha$	1040	18.15
$1_{11} \rightarrow 2_{12}$	M = 1	norm	520	33.98
$1_{10} \rightarrow 2_{11}$	M = 1	norm	1300	−155.94
	M = 0	norm	1300	5.42
$4_{04} \rightarrow 4_{13}$	M = 4	norm	1300	4.85

[a] $\mu_a = 1.1$, $\mu_b = 0.7$, $\mu_{total} = 1.3$ D.

attempted to estimate the unperturbed positions of ν_1 and ν_3 as well as their $^{14/15}N$ isotopic shifts $\Delta\nu_1$ and $\Delta\nu_3$, respectively, by use of the differences between calculated and measured frequencies of their combination bands, as described in ref 10. The corrections of $\Delta\nu_1$ and $\Delta\nu_3$ are calculated from the isotopic shifts of $\Delta(2\nu_2)$, $\Delta(\nu_2 + \nu_3)$, and $\Delta(\nu_4 + \nu_5)$, these values having been collected in Table VII. Because of the very pronounced intensity of the $2\nu_2$ band, we expect its resonance with ν_1 to be particularly strong. The resonances of ν_1 with $(\nu_2 + \nu_3)$ and of ν_3 with $(\nu_4 + \nu_5)$, respectively, in comparison seem to be of minor importance. We, therefore, transfer the correction for $\Delta(2\nu_2)$ (measured − calculated, Table VII) completely on to ν_1, whereas the corrections for $\Delta(\nu_2 + \nu_3)$ and $\Delta(\nu_4 + \nu_5)$ only contribute with a weight of 1/3.

In this way we obtain the following corrected values for the isotopic shifts in the Ar matrix for the species $F^{15}NNN$, $FN^{15}NN$, $FNN^{15}N$, respectively: $\Delta\nu_1 = 2.0$, 36.0, 26.0 cm^{-1}; $\Delta\nu_3 = 18.7$, 2.7, 0.4 cm^{-1}. The isotopic shifts for $\Delta(2\nu_3)$ divided by 2 (i.e., $\sim\Delta\nu_3$) yield 17.3, 2.5, 0.5 cm^{-1}, in good agreement with the corrected values above.

In order to compensate for matrix effects, the matrix values for the frequency shifts have been corrected according to:

$$\Delta(\text{gas}) = \Delta(\text{matrix})(1 - \delta\nu/\nu)$$

[11] where $\delta\nu$ is the frequency change gas/matrix. The (hypothetical) unperturbed ν_1 and ν_3 frequencies in the gas phase are estimated to be 2044 and 876 cm^{-1}, respectively. Finally, all isotopic shifts have been corrected for anharmonic contributions in order to fulfill the Teller–Redlich product rule.[10] The resulting parameters have been collected in Table VIII and are used for the normal coordinate analysis.

Because of the uncertainty in the corrections, the parameters involving ν_1 and ν_3 have been given reduced weights in the normal coordinate analysis, using the program NORCOR.[12] The input was: molecular geometry (Table III), corrected fundamental frequencies (Table VIII), isotopic frequency shifts, centrifugal distortion constants (Table I), and inertial defects in the ground and $v_5 = 1$ state. The harmonic force field was calculated iteratively, starting from an ab initio force field (see below). The harmonic force constants are shown in Table IX and the calculated frequencies as well as the rotation–vibration parameters shown with the corrected data in Table VIII.

Ab Initio Calculations. Ab initio calculations were performed using the GAUSSIAN 82 program[13] with 6-31G* basis set on a BASF 7/88 computer. In order to determine correlation effects, all geometries were fully optimized at the Hartree–Fock and second-order Møller–Plesset levels of theory, the latter apparently working exceedingly well for fluorinated compounds.[14] The geometrical parameters calculated at these levels are collected in Table X together with the experimental structure. Obviously the calculations at HF level underestimates the bond length of the FN bond considerably, whereas the calculations at MP2 level predicts this length rather accurately. Also the angles are well predicted (especially at MP2 level), whereas the predictions for the two NN bonds seem rather dubious at both levels. A test calculation on HN_3 using a 6-31G** basis set at the same levels of calculation yielded values for the structural parameters that vary in a similar way from the experimental data (see Table X). Since the molecular geometry calculated at the MP2 level is quite close to the experimental structure, it seems worthwhile to use the associated wave functions to calculate other electronic properties for FN_3 that can be compared with the experiment.

First of all, one can calculate the partial charges placed on the various atoms and the resulting dipole moment components. These data have been collected in Table XI. It is, furthermore, possible to calculate the forces acting between the various nuclei in the molecule and thus derive the appropriate force constants. This has been done for HN_3 and FN_3 at the MP2 level. These force fields and the corresponding fundamental frequencies have been collected in Table IX, which also includes other calculations on HN_3 showing the importance of including configuration interaction in these calculations. The $N_\beta N_\omega$ or more correctly, the asymmetric NNN stretching vibration, is consistently calculated too high, as

(10) Becher, H. J. Schnöckel, H. G.; Willner, H. *Z. Phys. Chem. (Frankfurt am Main)* **1974**, *92*, 33.
(11) Schnöckel, H. G. *J. Mol. Struct.* **1975**, *29*, 123.
(12) Christen, D. *J. Mol. Struct.* **1978**, *48*, 101.
(13) Binkley, J. S.; Frisch, M.; DeFrees, D. J.; Raghavachari, K.; Whiteside, R. A.; Schlegel, H. B.; Flueter, G.; Pople, J. A. Carnegie-Mellon Chemistry Publication Unit, Pittsburgh, PA, 1983.
(14) Mack, H. G.; Christen, D.; Oberhammer, H., to be published.
(15) Winnewisser, B. P. *J. Mol. Spectrosc.* **1980**, *82*, 220.
(16) Lievin, J.; Breulet, J.; Verhaegen, G. *Theor. Chim. Acta* **1979**, *52*, 75–88.
(17) Moore, C. B.; Rosengren, K. *J. Chem. Phys.* **1966**, *44*, 4108.

Table V Measured Vibrational Frequencies in FN_3 (cm^{-1})

gas-phase	Ar matrix					
FNNN	FNNN	$F^{15}NNN$	$FN^{15}NN$	$FNN^{15}N$	assignment	PED[b]
2171.5 s	2161.6	2124.9	2148.1	2147.0	$2\nu_2$	
		(36.7)[a]	(13.5)	(14.6)		
2037.0 vs	2031.0	2020.6	1999.4	2006.2	ν_1	100 N≡N + 12 N=N
		(10.4)	(31.6)	(24.8)		
1953.0 w	1947.4	1908.6	1938.8	1939.4	$\nu_2 + \nu_3$	
		(38.8)	(8.6)	(8.0)		
1736.0 vw	1728.5	1694.0	1723.6	1727.4	$2\nu_3$	
		(34.5)	(4.9)	(1.1)		
1090.0 m	1085.6	1062.5	1081.2	1078.8	ν_2	88 N=N
		(23.1)	(4.4)	(6.8)		
897.0 w	892.0	890.0	880.0	886.9	$\nu_4 + \nu_5$	
		(2.0)	(12.0)	(5.1)		
873.5 s	868.1	850.9	865.3	867.5	ν_3	80 NF + 25 FNN + 10 NNN
		(17.2)	(2.8)	(0.6)		
658.0 m	652.1	651.9	640.8	649.5	ν_4	29 NNN + 23 FNN + 15 NF
		(0.2)	(11.3)	(2.6)		
504.0 w	502.8	500.9	491.1	499.6	ν_6	100 oop
		(1.9)	(11.7)	(3.2)		
241.0 m	239.9	239.8	238.2	236.5	ν_5	66 FNN + 68 NNN
		(0.1)	(1.7)	(3.4)		

[a] Values in parentheses are ^{15}N isotopic shifts relative to FNNN in Ar matrix. [b] Potential energy distribution for the fundamental vibrations are calculated from the normal coordinate analysis (%).

Table VI. Frequency Differences (cm^{-1}) $2\nu_2 - \nu_1$, $\nu_1 - (\nu_2 + \nu_3)$, and $(\nu_4 + \nu_5) - \nu_3$ As a Probe of the Perturbation of ν_1 and ν_3

	FNNN	$F^{15}NNN$	$FN^{15}NN$	$FNN^{15}N$
$2\nu_2 - \nu_1$	131	105	149	141
$\nu_1 - (\nu_2 + \nu_3)$	84	112	61	67
$(\nu_4 + \nu_5) - \nu_3$	24	39	15	19

Table VII. Calculated and Measured Isotopic Shifts Relative to FNNN in $2\nu_2$, $(\nu_2 + \nu_3)$, and $(\nu_4 + \nu_5)$ According to Table V

	$F^{15}NNN$	$FN^{15}NN$	$FNN^{15}N$
$(2\nu_2)_{measd}$	36.7	13.5	14.6
$(2\nu_2)_{calcd}$	46.2	8.8	13.6
measd − calcd[a]	−9.5	4.7	1.0
$(\nu_2 + \nu_3)_{measd}$	38.8	8.6	8.0
$(\nu_2 + \nu_3)_{calcd}$	40.3	6.7	7.4
measd − calcd[a]	−1.5	1.9	0.6
$(\nu_4 + \nu_5)_{measd}$	2.0	12.0	5.1
$(\nu_4 + \nu_5)_{calcd}$	0.3	13.0	6.0
measd − calcd[a]	1.7	−1.0	−0.9

[a] Correction.

is the NX vibration (especially for NH), whereas all other vibrations are reproduced quite well.

We have also calculated the electric field gradients at the various nuclei, which in the case of nuclei possessing a quadrupole moment leads to quadrupole coupling and consequent hyperfine structure of the rotational transitions. This hyperfine structure has not been analyzed yet, but we include in Table XII the calculated coupling constants in the inertial axis frame, using the field gradients from the ab initio calculations and the quadrupole moment for ^{14}N from the determination of Winter and Andrä (1.9×10^{-26} cm^2).[18] This value of the ^{14}N quadrupole moment taken together with the calculated field gradients for ammonia and fluorinated amines reproduce the measured nuclear quadrupole coupling constants extremely well.[14] The coupling tensors are qualitatively identical at both levels of calculation and unequivocally show the coupling constants for N_α to be much larger than those for the other two positions in the N_3 chain, in concordance with the experimental findings.

Discussion

Having obtained information regarding structural and bonding properties of FN_3, it is now possible to compare these properties with those of other covalent azides or with compounds of the general type FN=Y (see Tables XIII and XIV). The characteristics of the FN_3 structure are the nonlinear N_3 chain, a particularly big difference in the bond lengths $N_\alpha N_\beta$ and $N_\beta N_\omega$ (δ = 12.1 pm), corresponding to a big difference in the appropriate force constants (viz. 17.4 versus 6.7 100 N/m), a very long NF bond (the corresponding force constant is extremely small, 3.75 100 N/m), and a noteworthy small FNN angle. The origin of these properties is probably best visualized by mesomeric structures I–V. Structure II deserves some consideration because fluorine

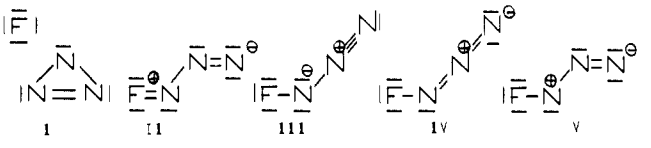

is potentially a strong π donor, but the experimental NF bond length is too long and the calculation of the partial charges does not allow for a positive charge on fluorine, so this structure must be discarded. Except for II, all other mesomeric structures seem to contribute to the properties of FN_3.

The very small FNN angle can be explained by implying structures I and III. The weakness of the FN and $N_\alpha N_\beta$ bonds can be inferred from structures I, III, and V. These structures also spotlight the ease with which the stable molecules NF and N_2 are produced, although the actual reasons for the breakup are the very low-lying antibonding N_β orbitals (~0.06 au) whose partial filling (from the only weakly binding N_α orbitals) radically weakens the $N_\alpha N_\beta$ bond.

Structures I and V explain the nonlinearity of the N_3 chain, and structures I, III, IV, and V taken together establish partial charges corresponding to those calculated ab initio. A comparison of the structural data of FN_3 with those of other covalent azides (Table XIII), considering their possible mesomeric forms, clearly shows FN_3 to be the thermally least stable of these (notably unstable) molecules, although the partial structure of the azide group is hardly changed from substituent to substituent, including the NNN angle, which seems to be close to 170° in all cases, where

(18) Winter, H.; Andrä, H. J. *Phys. Rev. A* **1980**, *21*, 581.
(19) Anderson, D. W. W.; Rankin, D. W. H.; Robertson, A. *J. Mol. Struct.* **1972**, *14*, 385.
(20) Christe, K. O.; Christen, D.; Oberhammer, H.; Schack, C. J. *Inorg. Chem.* **1984**, *23*, 4283.
(21) Cook, R. L.; Gerry, M. C. L. *J. Chem. Phys.* **1970**, *53*, 2525.
(22) Espoti, C. D.; Cazzoli, G.; Favero, P. G. *J. Mol. Spectrosc.* **1985**, *109*, 229.
(23) Kuczkowski, R. L.; Wilson, E. B., Jr. *J. Chem. Phys.* **1963**, *39*, 1030.
(24) Christen, D.; Oberhammer, H.; Hammaker, R. M.; Chang. S.-C.; Des Marteau, D. D. *J. Am. Chem. Soc.* **1982**, *104*, 6186.
(25) DeFrees, D. J.; Loew, G. H.; McLean, A. D. *Astrophys. J.* **1982**, *254*, 405–411.
(26) Sjogren, C. E.; Nielsen, C. J. *J. Mol. Struct.* **1986**, *142*, 285–290.

Table VIII. Corrected Gas-Phase Fundamental Frequencies and Isotopic Shifts (cm^{-1}) for the Normal Coordinate Analysis As Well As Centrifugal Distortion Constants (kHz) and Inertia Defects (u $Å^2$)

			$^{14/15}N$ isotopic shifts		
	FNNN		$F^{15}NNN$	$FN^{15}NN$	$FNN^{15}N$
ν_1	2044 (2044)[a]	$\Delta\nu_1$	2.0 (0.3)	36.0 (37.7)	26.0 (30.2)
ν_2	1090 (1090)	$\Delta\nu_2$	25.3 (24.6)	4.9 (4.5)	7.1 (6.9)
ν_3	876 (875)	$\Delta\nu_3$	18.7 (18.7)	2.7 (2.6)	0.4 (0.3)
ν_4	658 (657)	$\Delta\nu_4$	0.4 (0.1)	11.7 (12.4)	2.7 (2.8)
ν_5	241 (241)	$\Delta\nu_5$	0.3 (1.1)	1.8 (1.4)	3.5 (2.8)
ν_6	504 (507)	$\Delta\nu_6$	1.9 (1.8)	11.9 (11.8)	3.3 (3.4)
Δ_J	0.0024 (0.0045)		0.0025 (0.0044)	0.0024 (0.0045)	0.0024[b] (0.0042)
Δ_{JK}	−0.1465 (−0.1452)		−0.1272 (−0.1323)	−0.1287 (−0.1453)	−0.1465[b] (−0.1395)
Δ_K	3.2881 (3.2080)		3.2881[b] (2.8728)	3.2881[b] (3.2290)	3.2881[b] (3.1819)
δ_J	0.0009 (0.0010)		0.0011[b] (0.0010)	0.0009[b] (0.0010)	0.009[b] (0.0009)
δ_K	0.0348[b] (0.0256)		0.0348[b] (0.0252)	0.0348[b] (0.0252)	0.0348[b] (0.0248)
id	0.229 (0.022)		0.229[b] (0.223)	0.231[b] (0.222)	0.229[b] (0.224)
id (v_5 = 1)	0.548 (0.570)		0.548[b] (0.583)	0.548[b] (0.566)	0.548[b] (0.576)

[a] Values in parentheses are calculated from the best force field. [b] Not used in the fit.

Table IX. Force Fields and Vibrational Frequencies for HN_3 and FN_3[i]

fc	HN_3[a]	HN_3[b]	HN_3[c]	HN_3[d]	FN_3[e]	FN_3[f]	FN_3[g]
N≡N	21.9	22.50	18.64	16.00	24.26	19.83	17.414
N=N	9.3	7.24	11.17	9.86	7.72	8.34	6.686
N—X	7.1	6.75	7.08	6.757	6.30	4.66	3.753
NNN	0.38	0.79	0.75	0.729	0.46	0.52	0.477
XNN	0.71	1.13	0.74	0.611	1.98	1.47	1.245
oop	0.10	0.018	0.022		0.008	0.020	0.014
N≡N/N=N	2.4	2.36	−0.27	0.73	2.85	−0.78	1.985
N≡N/N—X		−0.14	−0.20		0.29	−0.01	−0.01[h]
N≡N/NNN	−0.14	−0.06	0.03		0.04	0.01	0.01[h]
N≡N/XNN		−0.06	−0.21		−0.37	−0.10	−0.01[h]
N=N/NX	−0.23	−0.01	−0.10		0.41	0.58	0.200
N=N/NNN	−0.35	0.29	0.38	0.838	0.16	0.18	0.100
N=N/XNN	1.1	1.17	0.97		0.82	0.50	0.682
NX/NNN		−0.03	0.03		0.04	0.03	0.192
NX/XNN	0.24	0.34	0.31		1.12	0.89	0.417
NNN/XNN	−0.02	0.09	0.09	0.048	0.17	0.21	0.200
			A′				
$\nu_{N\equiv N}$	2344	2330	2385	2150	2385	2394	2044
$\nu_{N=N}$	1617	1465	1263	1273	1226	1143	1090
ν_{NX}	3606	3488	3574	3324	1046	946	876
δ_{XNN}	982	1026	1132	1168	758	690	658
δ_{NNN}	472	599	555	527	282	253	241
			A″				
oop	496	683	581	588	606	499	504

[a] Reference 16, RHF/6-31G (GAUSSIAN 70). [b] Reference 26, DZ basis set (MOLECULE). [c] This work, MP2/6-31G**. [d] Reference 17, experimental. [e] This work, RHF/6-31G*. [f] This work, MP2/6-31G*. [g] This work, experimental. [h] Fixed, due to their very small Jacobian matrix elements. [i] Force constants in 10^2 N/m, bending force constants and bending–stretching constants normalized on 10^{-10} m, frequencies in cm^{-1}.

Table X. Molecular Structure of FN_3 and HN_3. Comparison of Experimental Structure with ab Initio HF and MP2 (6-31G* Basis Set for FN_3, 6-31G** Basis Set for HN_3) Calculations[d]

	FN_3			HN_3			CI
	r_s[a]	HF[a]	MP2[a]	r_s[b]	HF[a]	MP2[a]	(SD + Q)[c]
$N_\alpha X$	144.4	138.19	143.21	101.5	100.55	101.92	101.9
$N_\alpha N_\beta$	125.3	125.35	128.24	124.3	123.8	125.18	125.7
$N_\beta N_\omega$	113.2	109.95	115.41	113.4	109.87	115.91	113.9
$XN_\alpha N_\beta$	103.8	104.3	103.8	108.8	108.1	109.6	107.5
$N_\alpha N_\beta N_\omega$	170.9	174.1	171.6	171.3	173.9	171.1	172.4

[a] This work. [b] Reference 15. [c] Reference 25. [d] In pm and deg.

Table XI. Partial Charges (au) and Dipole Moment Components (D) in FN_3

	F	N_α	N_β	N_ω	μ_a	μ_b	μ_{total}
HF	−0.31	−0.13	+0.43	+0.01	1.49	−0.57	1.60
MP2	−0.31	−0.06	+0.33	+0.04	1.62	−0.44	1.68
exptl[a]					1.1	0.7	1.3

[a] See Discussion.

Table XII. Nuclear Quadrupole Coupling Constants (MHz) in the Inertial Principal Axis System of FN_3

	RHF/6-31G*			MP2/6-31G*		
χ	N_α	N_β	N_ω	N_α	N_β	N_ω
aa	6.65	−1.32	−0.33	6.42	−1.40	−0.04
bb	0.02	−0.51	3.26	0.33	−0.84	3.78
cc	−6.63	1.83	−2.93	−6.75	2.24	−3.74
ab	1.17	0.04	3.31	1.21	−0.11	3.20

Table XIII. Structural Parameters (ppm and deg) of Some Covalent Azides

	CH_3N_3[a]	CF_3N_3[b]	HN_3[c]	ClN_3[d]	FN_3[e]
X—N	146.8 (5)	142.5 (5)	101.5 (1.5)	174.5 (5)	144.4 (1.0)
N_α=N_β	121.6 (4)	125.2 (5)	124.3 (5)	125.2 (1.0)	125.3 (1.0)
N_β≡N_ω	113.0 (5)	111.8 (3)	113.4 (2)	113.3 (1.0)	113.2 (1.0)
∠XNN	116.8 (3)	112.4 (2)	108.8 (4.0)	108.7 (0.5)	103.8 (5)
∠NNN	180.[f]	169.6 (3.4)	171.3 (5.0)	171.9 (0.5)	170.9 (1.0)

[a] Reference 19, r_a values. [b] Reference 20, r_{av} values. [c] Reference 15, r_s values. [d] Reference 21, r_s/r_0 values. [e] This work, r_s values. [f] Assumed.

it could be determined. The main structural difference between the well-known covalent azides is the XNN angle, which differs by as much as 13° going from CH_3N_3 to FN_3. Table XIV shows how much NF bond lengths vary in the different compounds (the Pauling FN single bond length is 138 pm) depending on the Y fragment.

Table XIV. Structural Paramters of FN=Y Type Compounds

	Y =			
	O[a]	NF(cis)[b]	CF_2[c]	N_2[d]
F-N (pm)	151.6	138.4 (1.0)	138.9 (2)	144.4 (1.0)
(FNY (deg))	109.9	114.5 (0.5)	107.9 (2)	103.8 (0.5)

[a] Reference 22, r_e values. [b] Reference 23. [c] Reference 24, r_α^0 values. [d] This work.

Conclusion

We have succeeded in recording the microwave and IR spectra of gaseous triazadienyl fluoride with its ^{15}N-enriched isotopomers. The analysis of these spectra has established the molecular geometry (C_s symmetry) as well as the harmonic force field. The data have been interpreted on the basis of extended ab initio calculations, partially involving configuration interaction. The reason for the explosive nature of FN_3 is now well understood.

Acknowledgment. We thank the Deutsche Forschungsgemeinschaft and the Verband der Chemischen Industrie e.V.-Fonds der Chemie for financial support.

Registry No. FN_3, 14986-60-8; $F^{15}NNN$, 111999-52-1; $FN^{15}NN$, 111999-53-2; $FNN^{15}N$, 111999-54-3; N_2, 7727-37-9; $^{15}N_2$, 14390-96-6; HN_3, 7782-79-8; $Na^{15}NNN$, 111999-55-4; $NaN^{15}NN$, 111999-56-5.

In Situ FT-IR Investigation of Phospholipid Monolayer Phase Transitions at the Air-Water Interface

Melody L. Mitchell and Richard A. Dluhy*

Contribution from the National Center for Biomedical Infrared Spectroscopy, Battelle-Columbus Laboratories, 505 King Avenue, Columbus, Ohio 43201-2693. *Received June 19, 1987*

Abstract: The liquid-expanded to liquid-condensed phase transition of 1,2-dipalmitoyl-*sn-glycero*-3-phosphocholine (DPPC) monolayers at the air-water (A/W) interface has been investigated in situ with external reflectance Fourier transform infrared spectroscopy. Infrared spectra have also been obtained for monolayer films of 1,2-dimyristoyl-*sn-glycero*-3-phosphocholine (DMPC, a liquid-expanded film) and 1,2-distearoyl-*sn-glycero*-3-phosphocholine (DSPC, a liquid-condensed film). All three phospholipid monolayer films were monitored in the conformation-sensitive C-H stretching region as a function of molecular area at the air-water interface. The measured frequencies of the symmetric and antisymmetric CH_2 stretching bands for the DPPC monolayer in the high molecular area, expanded phase (2853 and 2924 cm^{-1}, respectively) are comparable to those of bulk DPPC multilayer dispersions above its main thermotropic phase transition and indicate a fluid and disordered conformation in the hydrocarbon chains. The measured frequencies for the low molecular area, condensed phase of DPPC (2849 and 2919 cm^{-1}) indicate a rigid, mostly all-trans hydrocarbon chain conformation for the condensed phase monolayer, similar to the low-temperature, gel phase bulk DPPC dispersion. A continuous decrease in frequency with decreasing molecular area is observed throughout the transition region for the DPPC monolayer. These results demonstrate that the DPPC monolayer transition is (a) heterogeneous and biphasic in character, with coexistence of fluid and solid phases, and (b) involves a conformational change in the hydrocarbon chains of the monolayer as the average molecular area is decreased in the transition region. These trends are supported by the data for the DMPC and DSPC monolayer films. Molecular orientations relative to the substrate are also discussed in light of band intensities in both the parallel and perpendicular polarized spectra.

Monomolecular films composed of synthetic phospholipids have been widely utilized as model systems in order to study the physical properties of biological membranes.[1-3] The usefulness of these monolayer systems (which are usually constructed via Langmuir-Blodgett techniques) stems from the fact that the experimenter is allowed a wide lattitude in choosing the composition and physical state of the molecules in the monolayers; as a result, a large variety of model systems can be investigated. Recent biophysical applications of these monolayer techniques have included antibody-hapten binding in model phospholipid membranes,[4-6] protein surface activity,[7] and the insertion of signal sequence peptides into phospholipid monolayers.[8,9]

Unfortunately, while phospholipid monolayers at the A/W interface have been extensively studied as models for membrane bilayers and interfacial phenomena, there is virtually no information available concerning the detailed physical structure of these systems.[10] The lack of information concerning the molecular-level structure of monolayers at the A/W interface can be traced to the inability of most spectroscopic techniques to study a low surface area, flat water interface with sufficient sensitivity to produce spectra with reasonable signal-to-noise ratios.[10] The spectroscopic techniques in use consisted mainly of visible absorption and, of late, fluorescence methods.[2,11] Conformationally sensitive vibrational spectroscopic techniques were limited to transferred films on reflective metal substrates.[9,12,13] Recently, however, we have used external reflection Fourier transform infrared spectroscopy to measure, in situ, the vibrational spectra of insoluble mono-

* Author to whom correspondence should be addressed.

(1) Phillips, M. C. In *Progress in Surface and Membrane Science*; Academic: New York, 1972; Vol. 5, p 139.
(2) Kuhn, H.; Mobius, D.; Bucher, N. In *Physical Methods in Chemistry*; Weissberger, A., Rossiter, B. W., Eds.; Wiley-Interscience: New York, 1972; Vol. I, Part 3B, p 577.
(3) Gershfeld, N. L. *Annu. Rev. Phys. Chem.* **1976**, *27*, 349.
(4) Hafeman, D. G.; von Tscharner, V.; McConnell, H. M. *Proc. Natl. Acad. Sci. U.S.A.* **1981**, *78*, 4552.
(5) Subramaniam, S.; Seul, M.; McConnell, H. M. *Proc. Natl. Acad. Sci. U.S.A.* **1986**, *83*, 1169.
(6) Uzgiris, E.; Kornberg, R. *Nature* (London) **1983**, *301*, 125.
(7) Fringeli, U. P.; Leutert, P.; Thurnhofer, H.; Fringeli, M.; Burger, M. *Proc. Natl. Acad. Sci. U.S.A.* **1986**, *838*, 1315.
(8) Briggs, M. S.; Gierasch, L. M.; Zlotnick, A.; Lear, J. D.; DeGrado, W. F. *Science* **1985**, *228*, 1096.
(9) Briggs, M. S.; Cornell, D. G.; Dluhy, R. A.; Gierasch, L. M. *Science* **1986**, *233*, 206.
(10) Mann, J. A. *Langmuir* **1985**, *1*, 10.
(11) Thompson, N. L.; McConnell, H. M.; Burghardt, T. P. *Biophys. J.* **1984**, *46*, 739.
(12) Okamura, E.; Umemura, J.; Takenaka, T. *Biochim. Biophys. Acta* **1985**, *812*, 139-146.
(13) Swalen, J. D.; Rabolt, J. F. In *Fourier Transform Infrared Spectroscopy. Application to Chemical Systems*; Ferraro, J. R., Basile, L. J., Eds.; Academic: New York, 1985; Vol. 4, p 283.

0002-7863/88/1510-0712$01.50/0